

Recent results of measuring black hole masses via reverberation mapping

Shai Kaspi

School of Physics and Astronomy and Wise Observatory, Raymond and Beverly Sackler
Faculty of Exact Sciences, Tel-Aviv University, Tel-Aviv 6997801, Israel
email: shai@wise.tau.ac.il

Abstract. Over the past three decades more than 100 Active Galactic Nuclei (AGNs) were measured using the reverberation mapping technique. This technique uses the response of the line emission in the Broad Line Region (BLR) to continuum emission variation and yields a measure for the distance of the BLR from the central Black Hole (BH). This in turn is used to measure the BH's mass. Almost all of these measurements are of low-luminosity AGNs while for quasars with luminosities higher than 10^{46} erg s⁻¹ there are hardly any attempts of reverberation mapping. This contribution reports on recent results from a two-decades campaigns to measure the BH mass in high-luminosity quasars using the reverberation mapping technique. BLR distance from the BH, BH mass, and AGN UV luminosity relations over eight orders of magnitude in luminosity are presented, pushing the luminosity limit to the highest point so far.

Keywords. galaxies: active, quasars: emission lines, galaxies: Seyfert

1. Introduction

Reverberation Mapping (RM) is a well developed method which is being used over the past three decades to measure the distance of the Broad Line Region (BLR) from the central black hole (BH) in Active Galactic Nuclei (AGNs), e.g., [Bahcall *et al.* \(1972\)](#); [Blandford & McKee \(1982\)](#); [Peterson \(1993, 2006\)](#); [Netzer & Peterson \(1997\)](#). This method uses the time lag between continuum variation of the AGN and the response Broad Line Region (BLR) emission line variation to estimate that distance. Once this distance is determined the AGN's central BH mass can be computed using the width of the emission line, and assumptions about the geometry of the BLR. Thus far, More than a hundred AGNs have sufficient data to significantly estimate the BLR size and the BH mass (e.g., [Kaspi *et al.* 2000, 2005](#); [Du *et al.* 2016](#); [Bentz & Katz 2015](#); [Grier *et al.* 2017](#)). These studies resulted with a firm relation between the BLR's size and the AGN's Luminosity, and a relation between the BH's mass and the AGN's Luminosity. Both relations are roughly consistent with that the size and the mass are scaling with the square root of the luminosity. These relations are widely used to estimate the BLR size and BH mass in thousands of AGNs using a single epoch spectrum, in order to study cosmological structure and scales, the mass function of AGNs, accretion history, etc.

Although these size–mass–luminosity relations are used for AGNs at all luminosities, RM studies have been limited until very recently to intermediate luminosity AGNs in the range $10^{44} < \lambda L_{\lambda}(5100\text{\AA}) < 10^{46}$ erg s⁻¹ and at low redshift, mostly $z < 0.5$. Most RM studies were carried out using the H β broad emission line which is conveniently located in the center of the optical wavelength region and is accessible for most optical spectrograph. In order to study if the size–mass–luminosity relations hold for higher-luminosity and higher-redshift AGNs there is a need to carry RM campaigns on such

objects. Though, due to the high redshift the $H\beta$ line is redshifted to the IR and the $C\text{IV}\lambda 1550$ and $\text{Ly}\alpha$ broad emission lines are redshifted to the optical region and can be used for RM with optical telescopes.

However, such studies are difficult to carry out due to a number of reasons: RM studies, specially toward high-luminosity and high-redshift AGNs, require a lot of telescope resources. Such objects have much larger BLR and much longer variability timescales, and thus need long monitoring periods - of order of a decade. Time Allocation Committees do not want to commit telescopes for such long periods. The light curves are smeared by the cosmic time dilution, and the continuum variations are smeared by the large BLR size, thus it is hard to detect the line variations in response to the continuum variations.

Because of these reasons only a few attempts were carried out so far to study RM of high-luminosity and high-redshift AGNs (e.g., [Welsh et al. 2000](#); [Trevese et al. 2007, 2014](#)). This contribution presents two RM studies carried out on these type of AGNs. Together with results from past and recently published studies, the size–mass–luminosity relations will be presented for the the $C\text{IV}\lambda 1550$ emission line over the whole luminosity range of AGNs.

2. Las Campanas Observatory, Chile, Campaign

We† monitored a sample of 17 quasars from the Calan-Tololo and the SDSS catalogs. The luminosities of the quasars in this sample are $\lambda L_{\lambda}(1350\text{\AA}) > 10^{46.5} \text{ erg s}^{-1}$ and their redshift range is $2.3 < z < 3.4$. Photometric observations were carried out using the 0.9m at the CTIO every about two months since 2005. Spectroscopic observations were carried out using the 2.5m DuPont telescope at LCO. The results from that decade long campaign are published in [Lira et al. \(2018\)](#). An example of a light curve and cross correlations to determine the time lags from the $C\text{IV}\lambda 1550$ and $\text{Ly}\alpha$ broad emission lines are shown in [Figure 1](#). In this study we significantly and reliably measure time lags for $\text{Ly}\alpha$ in 8 objects, for $C\text{IV}$ in 8 objects, for SiIV in 3 objects, and for $C\text{III]}$ in 1 object. Altogether significant time lags were measured for 10 distinct objects. We present an updated $C\text{IV}$ radius–luminosity relation in which the radius scales like the UV luminosity to the power of 0.46 ± 0.08 , and show for the first time a radius–luminosity relation for the other three lines. We conclude that the regions responsible for the emission of $\text{Ly}\alpha$, SiIV , $C\text{IV}$, and $C\text{III]}$ are commonly interior to that producing $H\beta$, but there is no clear stratification among them. Three out of the 17 sources in [Lira et al. \(2018\)](#) show an unexpected behavior in some emission lines in the sense that the line light curves do not appear to follow the observed UV continuum variations. This is an interesting behavior which is also seen in low luminosity AGNs (e.g., [Goad et al. 2016](#)).

3. HET—Wise Campaign

We‡ monitored a sample of 6 quasars in the luminosity range $10^{46} < \lambda L_{\lambda}(1350\text{\AA}) < 10^{48} \text{ erg s}^{-1}$ and redshift range of $2.3 < z < 3.4$. These objects are among the most luminous quasars and lie within the primary epoch of BH growth for luminous quasars. Photometric observations were carried out since 1994 at the 1m telescope of the Wise Observatory (Israel) for 18 years and spectroscopic observations were carried out since 1999 at the 9m Hobby-Eberly Telescope (HET) for 13 years. Preliminary results from that study were presented in [Kaspi et al. \(2007\)](#) where we show a preliminary $C\text{IV}$ time lag for S5 0836 + 71 at $z = 2.172$ of 188_{-37}^{+27} days in the rest frame.

† In collaboration with Paulina Lira, Ismael Botti, Hagai Netzer, Nidia Morrell, Julián Mejía-Restrepo, Paula Sánchez, Jorge Martínez, and Paula López.

‡ In collaboration with Niel Brandt, Dan Maoz, Hagai Netzer, Donald Schneider, Ohad Shemmer, and Kate Grier.

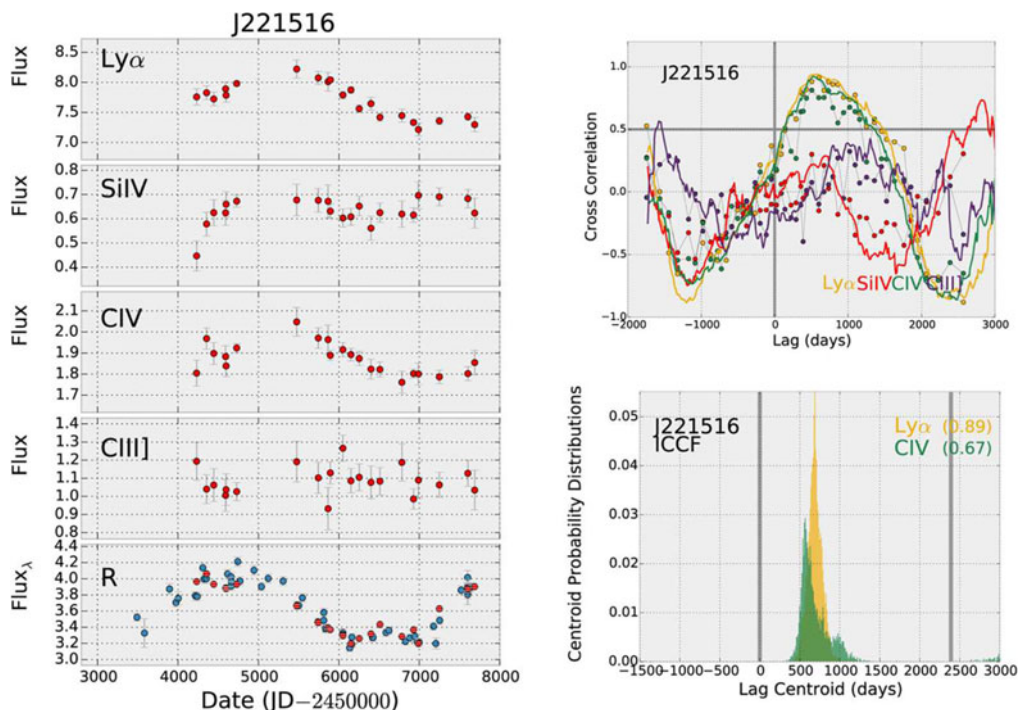


Figure 1. Continuum and emission lines light curves for the quasar 2QZ J221516 (left) together with cross correlation functions between the different emission lines and the continuum light curves (top right), and cross correlation centroid distribution for the two lines which show significant time lags (bottom right). For details see [Lira et al. \(2018\)](#).

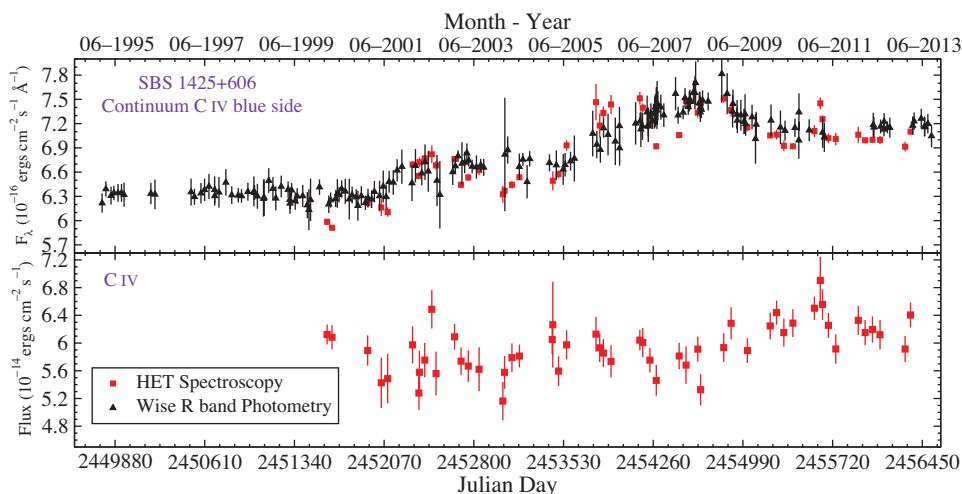


Figure 2. Continuum (top) and C IV (bottom) light curves of the quasar SBS 1425+606.

The results from the full period of this campaign will be presented in [Kaspi et al. \(2020, in preparation\)](#). An example of a light curve of one object is shown in [Figure 2](#). All objects in the sample show continuum variability of order 10%–70%. C IV time lags are detected for 3 objects and C III] time lag was detected in one object. The C IV time

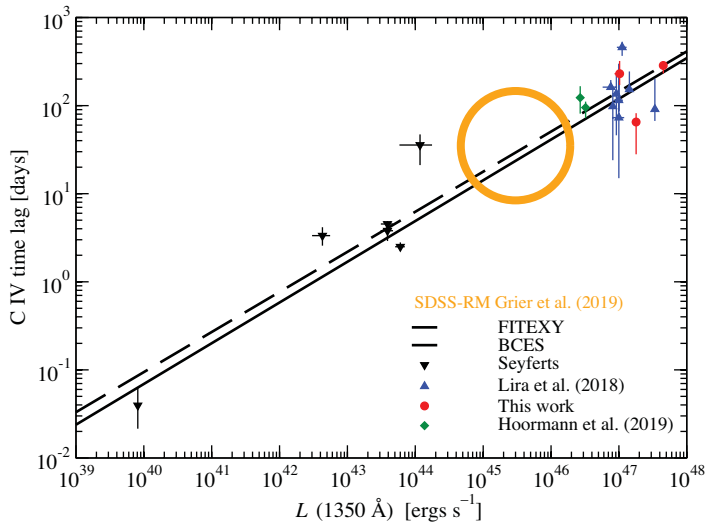


Figure 3. C IV time lag as a function of the UV luminosity.

lags are of order 100 to 250 light days. In the following we use these results together with results from previous studies to construct the relations between the BLR distance from the BH, BH mass, and AGN UV luminosity.

4. C IV Size–Mass–Luminosity Relations

C IV RM studies were carried out during the past three decades toward several low luminosity AGNs (Seyfert Galaxies), e.g., Peterson *et al.* (2004, 2005), De Rosa *et al.* (2015), Metzroth *et al.* (2006). Hoormann *et al.* (2019) report C IV RM time lags for two objects from the Dark Energy Survey Supernova Program (DES-SN) and the Australian Dark Energy Survey (OzDES) at redshifts of 1.9 and 2.6. In that study the photometric monitoring covers five years while the spectroscopic monitoring was 3–4 years. Out of the 393 objects with C IV in their sample, 23 were variable and had high cadence data but only two had significant time-lag measurements. These objects have 1350 Å luminosity of a few 10^{46} erg s $^{-1}$. Recently, Grier *et al.* (2019) report on C IV time lags in 52 AGNs from the Sloan Digital Sky Survey RM Project, with an estimated false-positive detection rate of 10%. 18 of these AGNs are defined as their “gold sample” with the highest-confidence lag measurements. These objects have redshift range of $1.4 < z < 2.8$ and luminosity range of $10^{44.5} < \lambda L_{\lambda}(1350\text{Å}) < 10^{45.6}$ erg s $^{-1}$. Adding all these results to the ones presented here, in the previous two sections, a size–luminosity relation can be determined between the C IV time lags and the 1350 Å luminosity. That relation is presented in Figure 3 and the fitted relation has a slope of 0.46 ± 0.03 , and an intercept of 0.17 ± 0.04 . This result is consistent with that measured by Lira *et al.* (2018).

The central masses of AGNs can be estimated using $M_{BH} = fG^{-1}V^2r$, where V is an estimate of the velocity of the BLR around the central mass, and r is an estimate of the typical distance between the BLR and the central BH. f is a scaling factor which depends on the BLR geometry and velocity field. Although it was found that using the C IV line to estimate the BH mass in AGNs has some drawbacks and limitations (e.g., Baskin & Laor 2005; Trakhtenbrot & Netzer 2012), we do present here BH mass–UV luminosity relation for this whole sample, since for the high-luminosity AGN we only have RM measurements of C IV. This relation is shown in Figure 4 and the fitted relation has a slope of 0.49 ± 0.06 , and an intercept of $0.88^{+0.57}_{-0.34}$.

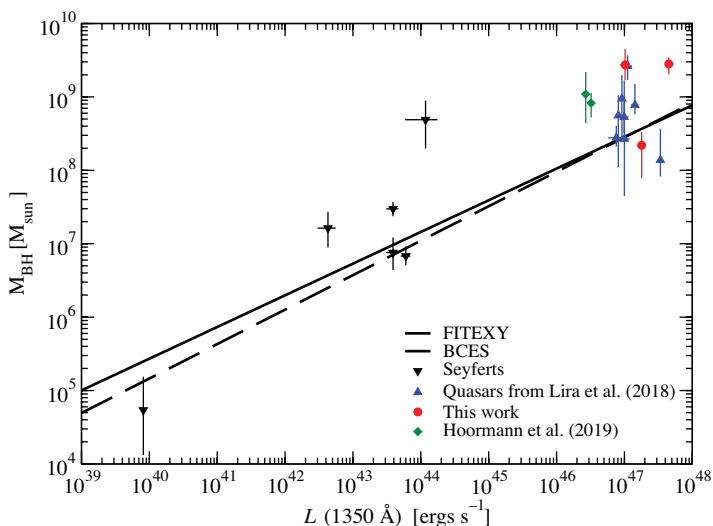


Figure 4. BH mass as a function of the UV luminosity for the sample of AGNs with measured C IV time lag.

The results presented here about RM of the C IV broad emission line, together with some recent similar studies, have populated the high-luminosity end of the size—mass—luminosity relations in AGNs (Kaspi *et al.* 2020, in preparation). We find that both the BH mass and the distance of the C IV emitting region from the BH, are scaling as the square root of the UV luminosity, to within the uncertainties. However, the low luminosity end at $\lambda L_{\lambda}(1350\text{\AA}) < 10^{43} \text{ erg s}^{-1}$ is poor with data points and further RM of the C IV line in low-luminosity AGNs are needed to better populate that region.

References

- Bahcall, J. N., Kozlovsky, B.-Z., & Salpeter, E. E. 1972, *ApJ*, 171, 467
 Baskin, A. & Laor, A. 2005, *MNRAS*, 356, 1029
 Bentz, M. C. & Katz, S. 2015, *PASP*, 127, 67
 Blandford, R. D. & McKee, C. F. 1982, *ApJ*, 255, 419
 De Rosa, G., Peterson, B. M., Ely, J., *et al.* 2015, *ApJ*, 806, 128
 Du, P., Lu, K.-X., Zhang, Z.-X., *et al.* 2016, *ApJ*, 825, 126
 Goad, M. R., Korista, K. T., De Rosa, G., *et al.* 2016, *ApJ*, 824, 11
 Grier, C. J., Trump, J. R., Shen, Y., *et al.* 2017, *ApJ*, 851, 21 (erratum 868, 76 [2018])
 Grier, C. J., Shen, Y., Horne, K., *et al.* 2019, *ApJ*, 887, 38
 Hoormann, J. K., Martini, P., Davis, T. M., *et al.* 2019, *MNRAS*, 487, 3650
 Kaspi, S., Smith, P. S., Netzer, H., Maoz, D., Jannuzi, B. T., & Giveon, U. 2000, *ApJ*, 533, 631
 Kaspi, S., Maoz, D., Netzer, H., Peterson, B. M., Vestergaard, M., & Jannuzi, B. T. 2005, *ApJ*, 629, 61
 Kaspi, S., Brandt, W. N., Maoz, D., Netzer, H., Schneider, D. P., & Shemmer, O. 2007, *ApJ*, 659, 997
 Lira, P., Kaspi, S., Netzer, H., *et al.* 2018, *ApJ*, 865, 56
 Metzroth, K. G., Onken, C. A., & Peterson, B. M. 2006, *ApJ*, 647, 901
 Netzer, H. & Peterson, B. M. 1997, in D. Maoz, A. Sternberg and E. Leibowitz (eds.), *Astronomical Time Series*, (Dordrecht: Kluwer Academic Publishers), p. 85
 Peterson, B. M. 1993, *PASP*, 105, 247
 Peterson, B. M., Ferrarese, L., Gilbert, K. M., *et al.* 2004, *ApJ*, 613, 682

- Peterson, B. M., Bentz, M. C., Desroches, L.-B., *et al.* 2005, *ApJ*, 632, 799 (erratum 641, 638 [2006])
- Peterson, B. M. 2006, in C. M. Gaskell, I. M. McHardy, B. M. Peterson and S. G. Sergeev (eds.) *AGN Variability from X-Rays to Radio Waves*, (Astronomical Society of the Pacific Conference Series) 360, 191
- Saturni, F. G., Trevese, D., Vagnetti, F., Perna, M., & Dadina, M. 2016, *A&A*, 587, A43
- Trakhtenbrot, B. & Netzer, H. 2012, *MNRAS*, 427, 3081
- Trevese, D., Paris, D., Stirpe, G. M., Vagnetti, F., & Zitelli, V. 2007, *A&A*, 470, 491
- Trevese, D., Perna, M., Vagnetti, F., Saturni, F. G., & Dadina, M. 2014, *ApJ*, 795, 164
- Welsh, W., Robinson, E. L., Hill, G., *et al.* 2000, *BAAS*, 32, 1458